Energy 162 (2018) 136–147

Contents lists available at ScienceDirect

Energy

journal homepage: www.elsevier.com/locate/energy

# Relationship between erythemal UV and broadband solar irradiation at high altitude in Northwestern Argentina

M.P. Utrillas [a], M.J. Marín [b], A.R. Esteve [c], G. Salazar [d, e], H. Suárez [d], S. Gandía [a], J.A. Martínez-Lozano [a, *]

[a] Solar Radiation Group, Departament de Física de la Terra i Termodinàmica, Universitat de València, Spain
[b] Solar Radiation Group, Departament de Matemàtiques per a l'Economia i l'Empresa, Universitat de València, Spain
[c] Solar Radiation Group, Departament de Didàctica de les Ciències Experimentals i Socials, Universitat de València, Spain
[d] Departamento de Física, Universidad Nacional de Salta, Salta Capital, Argentina
[e] Instituto de Investigaciones en Energía No Convencional (INENCO-CONICET), Salta Capital, Argentina

ARTICLE INFO

*Article history:*
Received 14 March 2018
Received in revised form
4 July 2018
Accepted 3 August 2018
Available online 3 August 2018

*Keywords:*
Erythemal ultraviolet irradiation
Broadband solar irradiation
Clearness indices
High altitude
Southern hemisphere

ABSTRACT

An analysis of the broadband solar irradiation, $I_T$, and the erythemal UV irradiation, $I_{UVER}$, has been performed using the measurements made from 2013 to 2015 at three sites located at altitudes over 1000 m a.s.l. In Northwestern Argentina (Salta, El Rosal, and Tolar Grande). The main objective of this paper is to determine a relationship between $I_T$ and $I_{UVER}$, which would allow to estimate $I_{UVER}$ from $I_T$ in places with few $I_{UVER}$ measurements available, and especially in those where is important to establish adequate photoprotection measures given their dense population and location at high altitude. The relationship between the daily values of $I_{UVER}$ and $I_T$ has been fitted to a linear regression ($I_{UVER} = m\ I_T + n$), showing good correlation in the three measurement sites ($R^2 \geq 0.77$). Besides, the $I_{UVER}/I_T$ ratio shows an increase with altitude of $0.32 \pm 0.03$ units per km, indicating a more significant influence of altitude on $I_{UVER}$ than on $I_T$. Total ozone column also attenuates more $I_{UVER}$ than $I_T$. In order to reduce the local nature of the relationship between $I_{UVER}$ and $I_T$, the clearness indices $k_T$ and $k_{TUVER}$ have been used to obtain a multivariable linear regression of $k_{TUVER}$ as a function of the solar zenith angle, $\theta_z$, and $k_T$, which shows good correlation ($R^2 \geq 0.89$) for the three measurement sites.



## 1. Introduction

Ultraviolet (UV) radiation, covering the wavelength range between 100 and 400 nm, represents a small fraction of the solar electromagnetic spectrum that reaches the top of the atmosphere with less intensity (about 8% of the total) than the visible and infrared parts of the solar spectrum [1]. It causes harmful effects on living beings [2,3] and terrestrial and marine ecosystems [4], as well as building materials such as plastics [5] or paints [6]. From an energetic point of view, the interest on UV radiation lies in the promising technology of catalytic detoxification for the disinfection and detoxification of water and wastewater [7–10].

On human beings, the effects of UV radiation are mainly observed over the skin [11,12], the eyes [13,14], and the immune system [15,16]. It also exits epidemiological evidence of the direct influence of sunlight over skin cancer in human beings [17,18]. The study of the effects of UV radiation over the skin is usually based on the ultraviolet erythemal radiation (UVER), which is determined as the spectrally integrated weighted solar irradiance at ground level with the spectral standard erythema action curve adopted by the CIE (Commission Internationale de l'Éclairage) in 1987 [19].

Although UV radiation is measured in many sites around the world, when these measurements are not available, it can usually be estimated from other radiometric or meteorological parameters. Several authors have proposed methods to do this [20–30], especially in the Northern Hemisphere. In these, a relationship is usually established between UV radiation, broadband solar radiation, and other atmospheric parameters such as the total column ozone, the aerosol extinction or cloudiness, adjusting it to the measurement

* Corresponding author. Departament de Física de la Terra i Termodinàmica, Facultat de Física, Universitat de València. Dr. Moliner 50, 46100 Burjassot, Valencia, Spain.
*E-mail address:* jmartine@uv.es (J.A. Martínez-Lozano).

https://doi.org/10.1016/j.energy.2018.08.021

site with an empirical model or by using radiative transfer models. All the studies previously cited have been performed in sites located at low altitudes (below 1000 m a.s.l.), with the exception of Esfaran (Iran), which is located at 1590 m a.s.l [26]. However, there are fewer studies relating these two spectral ranges in the Southern Hemisphere [31–33], which makes necessary, from the point of view of photoprotection, its analysis given the high population density and orographic characteristics of some regions, with high altitude zones such as the Altiplano in South America [34].

This article presents an analysis of the measurements of the UV erythemal irradiation ($I_{UVER}$) and the broadband solar irradiation ($I_T$) and the relationship between them. $I_{UVER}$ and $I_T$ have been used to estimate the clearness indices $k_{TUVER}$ and $k_T$, as well as the relationship between them, which are also analyzed here. Measurements were made from 2013 to 2015 at three different sites located in the Salta Province in Northwestern Argentina at high altitudes between 1190 and 3560 m a.s.l (Table I) [35]. The Salta Province, which covers an area of 154775 km$^2$, borders to the north with Bolivia and Paraguay and to the west with Chile. It has a total population of 1333000 inhabitants. The Salta Province has a wide diversity of landscapes, including high mountains, plateaus, valleys and plains, which determine different climate types.

### 1.1. Measurements

The $I_{UVER}$ measurements were made using Kipp & Zonen UVS-E-T radiometers in three measurement sites: Salta, El Rosal, and Tolar Grande. These instruments measure ultraviolet erythemal irradiance to the ISO 17166:1999, CIE S 007/E-1998 response function [1]. The UVS-E-T radiometers were compared at the University of Valencia (Spain) with a YES UVB-1 radiometer, calibrated previously in the National Institute for Aerospace Technology (INTA) in Spain. The calibration of the YES UVB-1 radiometer consists in the measurement of its spectral and cosine responses indoors as well as a comparison with a reference spectroradiometer outdoors. The result is a double input matrix that depends on the zenith angle and total column ozone [36]. However, the calibration of the UVS-E-T radiometers by direct comparison with the YES UVB-1 does not include the cosine factor of these instruments.

The $I_T$ measurements were made using an Eppley PSP in Salta and Kipp & Zonen CMP3 radiometers in El Rosal and Tolar Grande. The Eppley PSP is a first class pyranometer that measures solar radiation in the spectral range 285–2800 nm. Its temperature dependence is 1% over −20 °C to +40 °C. The cosine response of this instrument is 1% for 0–70° from zenith; 3% from 70 to 80°, according to the manufacturer's specifications. The CMP3 is a second class pyranometer that measures solar radiation in the spectral range 300–2800 nm. The temperature range of this instrument is from −40 °C to +80 °C, and its stability is better than 1% per year, according to the manufacturer's specifications. Both the PSP and the CMP3 were calibrated by comparison against a Kipp & Zonen CM-21 radiometer, which acted as reference instrument and had previously been calibrated against the Argentine reference standard, which is traceable to international calibration campaigns held at the World Radiation Centre (WRC) in Davos (Switzerland).

Data were registered every 5 s using Campbell Scientific CR1000

**Table 1**
Geographical coordinates of the measurement sites.

| Station | Latitude (°S) | Longitude (°W) | Altitude (m a.s.l.) |
|---|---|---|---|
| Salta | 24.785 | 65.412 | 1190 |
| El Rosal | 24.392 | 65.767 | 3355 |
| Tolar Grande | 24.590 | 67.450 | 3560 |

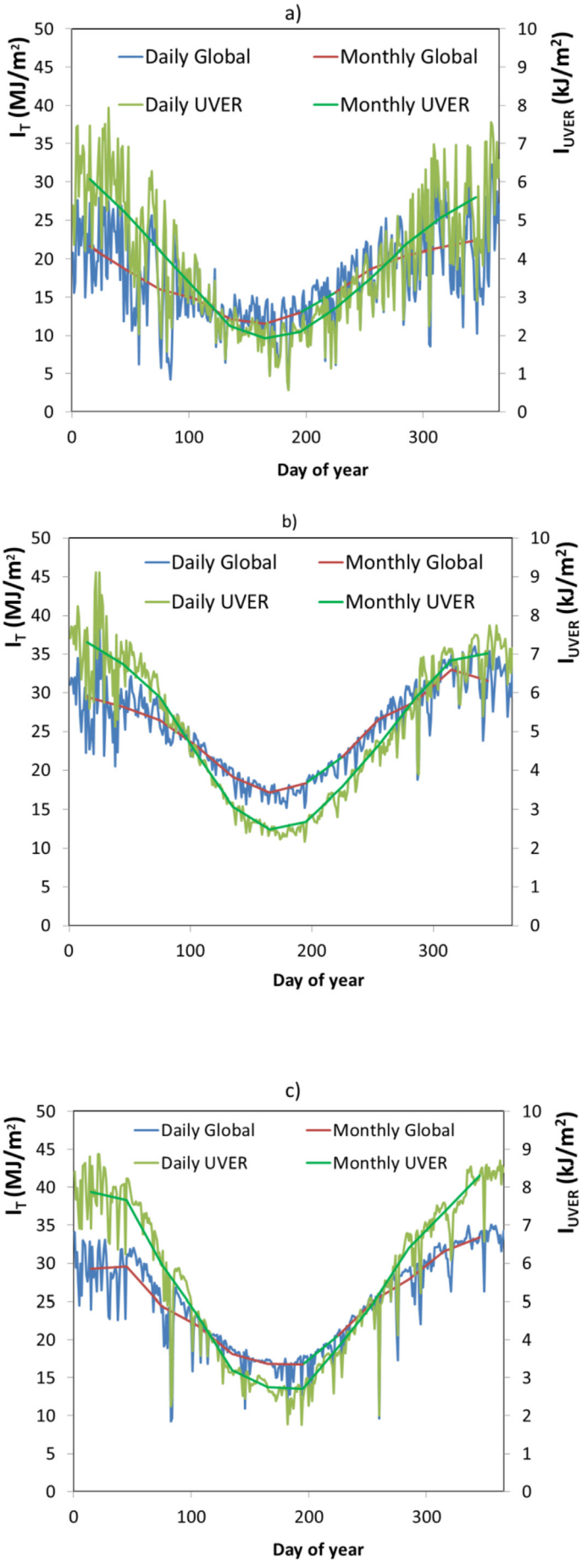


**Fig. 1.** Annual evolution of the daily and monthly mean values of $I_T$ (in MJm$^{-2}$) and $I_{UVER}$ (in kJm$^{-2}$) in: a) Salta, b) El Rosal, and c) Tolar Grande.

dataloggers, and 1 min averages of those measurements were recorded and used to obtain the hourly, daily and monthly averages presented in this study. Due to the cosine errors of the measurement instruments, especially for high solar zenith angles [37], only $I_T$ and $I_{UVER}$ measurements obtained for SZA < 70° have been used here. The hourly values can either be expressed in irradiance units ($W \cdot m^{-2}$) or irradiation units ($J \cdot m^{-2}$). The daily values are expressed in $J \cdot m^{-2}$.

## 2. Results and discussions

### 2.1. Analysis of $I_T$ and $I_{UVER}$

The annual evolution of the daily and monthly mean values of $I_T$ (in $MJ \cdot m^{-2}$) and $I_{UVER}$ (in $kJ \cdot m^{-2}$) in each measurement site: a) Salta, b) El Rosal, and c) Tolar Grande is shown in Fig. 1. For both $I_T$ and $I_{UVER}$, the evolution of the daily values shows symmetry respect to a central annual minimum in June (Salta and El Rosal) or July (Tolar Grande). Besides, strong variability is observed on the evolution of the daily values of $I_T$ and $I_{UVER}$ in Salta. However, this variability is less strong in the other two measurement sites, decreasing with the altitude, which could be explained by the different types of climate of the measurement sites: Salta has a humid subtropical climate (Cfa), while El Rosal and Tolar Grande have a cold desert climate (Bwk). Therefore, the main causes for the attenuation of solar radiation (cloudiness, water vapor, aerosols) have different characteristics. Altitude also has a big impact in the climate of the measurement sites.

Tables II and III show the most representative statistical indices (mean, standard deviation, standard error, median, minimum, maximum, 1st and 3rd quartiles, and 5th and 95th percentiles) of $I_T$ (in $MJ \cdot m^{-2}$) and $I_{UVER}$ (in $kJ \cdot m^{-2}$) for each month and the whole year in each measurement site.

The $I_T$ mean values vary from 11.5 to 22.3 $MJ\,m^{-2}$ in Salta, 17.1–33 $MJ\,m^{-2}$ in El Rosal, and 16.7–33.4 $MJ\,m^{-2}$ in Tolar Grande. These are considerably higher in El Rosal and Tolar Grande than those obtained in Salta: 27–39% in El Rosal and 22–37% in Tolar Grande. The maximum mean values are observed in December (Salta and Tolar Grande) and November (El Rosal), whereas the minimum mean values are observed in June (Salta and El Rosal) and July (Tolar Grande). The values of the mean and the median are similar, with the difference between them being always less than 9% of the mean value. The standard deviation shows values of 4.4 $MJ\,m^{-2}$ (25% of the mean value) in Salta, 2.1 $MJ\,m^{-2}$ (8%) in El Rosal, and 2.4 $MJ\,m^{-2}$ (10%) in Tolar Grande. The values of the standard deviation and the difference between the mean and the median are much higher in Salta than in the other two measurement sites, which indicates that atmospheric attenuation factors, such as cloudiness or aerosols, are more significant in Salta than in the other two measurement sites.

When comparing the extreme values (minimum and maximum) of $I_T$ with their corresponding quartile values ($Q_1$ and $Q_3$), the differences are always much higher in Salta than the other two measurement sites. The differences between the $Q_1$ and the

**Table 2**
Statistical indices of $I_T$ (in $MJ \cdot m^{-2}$) in: a) Salta, b) El Rosal, and c) Tolar Grande.

| | Mean ($MJ/m^2$) | Median ($MJ/m^2$) | σ ($MJ/m^2$) | Eσ ($MJ/m^2$) | Min ($MJ/m^2$) | Q1 ($MJ/m^2$) | Q3 ($MJ/m^2$) | Max ($MJ/m^2$) | P5 ($MJ/m^2$) | P95 ($MJ/m^2$) |
|---|---|---|---|---|---|---|---|---|---|---|
| (a) Salta | | | | | | | | | | |
| January | 21.6 | 20.8 | 4.3 | 0.8 | 15.0 | 17.6 | 25.3 | 27.9 | 15.5 | 27.5 |
| February | 18.7 | 18.6 | 5.6 | 1.1 | 6.2 | 13.7 | 23.5 | 26.9 | 10.8 | 26.7 |
| March | 16.0 | 16.4 | 6.6 | 1.2 | 4.2 | 11.6 | 21.6 | 25.6 | 5.8 | 24.7 |
| April | 14.8 | 13.9 | 2.6 | 0.5 | 11.7 | 12.6 | 16.5 | 20.1 | 12.1 | 19.4 |
| May | 12.2 | 12.1 | 2.3 | 0.4 | 6.4 | 11.3 | 13.3 | 18.7 | 8.8 | 15.0 |
| June | 11.5 | 12.5 | 3.0 | 0.6 | 4.8 | 9.1 | 14.1 | 15.2 | 6.7 | 15.0 |
| July | 13.0 | 13.5 | 3.4 | 0.6 | 2.8 | 11.4 | 15.3 | 17.2 | 6.2 | 16.5 |
| August | 15.6 | 16.4 | 3.9 | 0.7 | 6.2 | 14.0 | 18.3 | 21.1 | 6.7 | 20.1 |
| September | 18.7 | 17.6 | 3.7 | 0.7 | 10.9 | 16.1 | 21.5 | 25.2 | 12.8 | 23.6 |
| October | 20.4 | 20.9 | 4.7 | 0.8 | 11.4 | 16.1 | 25.1 | 29.5 | 14.2 | 26.7 |
| November | 21.4 | 21.0 | 6.5 | 1.2 | 8.6 | 16.7 | 27.1 | 30.8 | 9.8 | 30.6 |
| December | 22.3 | 22.0 | 5.9 | 1.1 | 10.3 | 17.3 | 27.5 | 32.3 | 14.3 | 31.1 |
| (b) El Rosal | | | | | | | | | | |
| January | 29.5 | 29.6 | 4.4 | 0.8 | 21.8 | 26.8 | 32.0 | 38.6 | 22.2 | 36.3 |
| February | 28.2 | 28.5 | 2.7 | 0.5 | 20.5 | 27.1 | 29.9 | 32.2 | 22.8 | 31.9 |
| March | 26.4 | 26.5 | 1.9 | 0.3 | 23.2 | 25.0 | 28.1 | 29.4 | 23.5 | 29.3 |
| April | 23.1 | 23.1 | 1.5 | 0.3 | 20.1 | 21.8 | 24.1 | 25.7 | 21.2 | 25.5 |
| May | 19.1 | 19.4 | 1.6 | 0.3 | 15.7 | 18.1 | 20.3 | 21.4 | 16.5 | 21.4 |
| June | 17.1 | 17.1 | 1.0 | 0.2 | 15.2 | 16.2 | 18.0 | 18.7 | 15.8 | 18.5 |
| July | 18.3 | 18.6 | 1.2 | 0.2 | 15.2 | 17.5 | 19.3 | 19.9 | 16.4 | 19.7 |
| August | 21.7 | 21.9 | 1.5 | 0.3 | 19.0 | 20.7 | 22.9 | 24.2 | 19.3 | 24.1 |
| September | 26.6 | 26.7 | 1.7 | 0.3 | 23.7 | 25.2 | 27.8 | 29.5 | 24.2 | 29.4 |
| October | 28.9 | 30.0 | 3.2 | 0.6 | 18.8 | 28.0 | 30.8 | 32.7 | 22.2 | 31.9 |
| November | 33.0 | 33.4 | 2.0 | 0.4 | 28.0 | 31.6 | 34.3 | 36.0 | 29.5 | 35.5 |
| December | 31.6 | 32.1 | 2.8 | 0.5 | 23.8 | 29.7 | 33.4 | 35.4 | 26.6 | 35.1 |
| (c)Tolar Grande | | | | | | | | | | |
| January | 29.3 | 29.4 | 3.2 | 0.6 | 22.7 | 27.6 | 32.0 | 34.1 | 23.5 | 33.0 |
| February | 29.5 | 30.0 | 2.3 | 0.4 | 22.6 | 28.7 | 31.0 | 32.0 | 24.4 | 31.9 |
| March | 24.4 | 25.8 | 4.9 | 0.9 | 9.2 | 23.4 | 27.2 | 29.9 | 14.3 | 29.5 |
| April | 21.9 | 22.0 | 2.3 | 0.4 | 15.8 | 20.7 | 23.4 | 25.3 | 16.9 | 24.9 |
| May | 18.2 | 18.5 | 2.1 | 0.4 | 10.9 | 17.8 | 19.3 | 20.6 | 14.5 | 20.6 |
| June | 16.8 | 17.1 | 0.7 | 0.1 | 14.7 | 16.5 | 17.3 | 17.6 | 15.0 | 17.5 |
| July | 16.7 | 17.5 | 2.0 | 0.4 | 12.0 | 16.5 | 17.9 | 18.8 | 12.7 | 18.7 |
| August | 20.6 | 20.5 | 2.1 | 0.4 | 14.3 | 19.3 | 22.5 | 23.2 | 17.0 | 23.1 |
| September | 25.0 | 25.4 | 3.3 | 0.6 | 9.6 | 24.2 | 26.9 | 28.6 | 22.3 | 27.9 |
| October | 27.8 | 28.9 | 3.1 | 0.6 | 17.3 | 27.5 | 29.6 | 31.3 | 21.6 | 30.7 |
| November | 31.6 | 32.1 | 1.7 | 0.3 | 26.2 | 30.8 | 32.7 | 33.2 | 28.1 | 33.1 |
| December | 33.4 | 33.8 | 1.6 | 0.3 | 26.3 | 32.8 | 34.3 | 35.0 | 31.6 | 34.9 |

**Table 3**
Statistical indices of $I_{UVER}$ (in $kJ \cdot m^{-2}$) in: a) Salta, b) El Rosal, and c) Tolar Grande.

| | Mean ($kJ/m^2$) | Median ($kJ/m^2$) | σ ($kJ/m^2$) | Eσ ($MJ/m^2$) | Min ($kJ/m^2$) | Q1 ($kJ/m^2$) | Q3 ($kJ/m^2$) | Max ($kJ/m^2$) | P5 ($kJ/m^2$) | P95 ($kJ/m^2$) |
|---|---|---|---|---|---|---|---|---|---|---|
| (a)Salta | | | | | | | | | | |
| January | 6.1 | 5.8 | 1.1 | 0.2 | 4.2 | 5.4 | 7.0 | 7.9 | 4.3 | 7.5 |
| February | 5.2 | 5.5 | 1.3 | 0.2 | 2.0 | 4.2 | 6.2 | 7.1 | 3.4 | 6.9 |
| March | 4.2 | 4.6 | 1.3 | 0.2 | 1.6 | 3.2 | 5.1 | 6.3 | 2.1 | 6.0 |
| April | 3.2 | 3.1 | 0.5 | 0.1 | 2.4 | 2.8 | 3.7 | 4.2 | 2.5 | 4.1 |
| May | 2.2 | 2.2 | 0.4 | 0.1 | 1.4 | 2.0 | 2.4 | 3.4 | 1.8 | 2.8 |
| June | 1.9 | 2.1 | 0.4 | 0.1 | 0.9 | 1.6 | 2.3 | 2.5 | 1.2 | 2.4 |
| July | 2.1 | 2.1 | 0.5 | 0.1 | 0.6 | 1.9 | 2.5 | 2.8 | 1.1 | 2.7 |
| August | 2.7 | 2.8 | 0.7 | 0.1 | 1.1 | 2.4 | 3.2 | 3.8 | 1.4 | 3.5 |
| September | 3.5 | 3.4 | 0.7 | 0.1 | 2.1 | 3.0 | 4.1 | 4.7 | 2.6 | 4.4 |
| October | 4.4 | 4.3 | 1.0 | 0.2 | 2.4 | 3.8 | 5.0 | 6.3 | 2.9 | 5.9 |
| November | 5.1 | 5.1 | 1.3 | 0.2 | 2.2 | 4.2 | 6.0 | 7.0 | 2.9 | 6.9 |
| December | 5.6 | 5.5 | 1.2 | 0.2 | 2.9 | 4.6 | 6.7 | 7.6 | 4.0 | 7.3 |
| (b) El Rosal | | | | | | | | | | |
| January | 7.3 | 7.3 | 0.9 | 0.2 | 5.6 | 6.8 | 7.8 | 9.1 | 5.8 | 8.9 |
| February | 6.7 | 6.9 | 0.6 | 0.1 | 5.1 | 6.6 | 7.1 | 7.5 | 5.5 | 7.3 |
| March | 5.9 | 5.8 | 0.6 | 0.2 | 5.0 | 5.4 | 6.4 | 6.8 | 5.1 | 6.6 |
| April | 4.4 | 4.4 | 0.5 | 0.1 | 3.6 | 4.1 | 4.9 | 5.2 | 3.7 | 5.2 |
| May | 3.1 | 3.1 | 0.4 | 0.1 | 2.4 | 2.8 | 3.3 | 3.7 | 2.5 | 3.6 |
| June | 2.5 | 2.5 | 0.1 | 0.1 | 2.2 | 2.4 | 2.6 | 2.7 | 2.3 | 2.7 |
| July | 2.7 | 2.7 | 0.3 | 0.1 | 2.2 | 2.5 | 2.8 | 3.2 | 2.3 | 3.1 |
| August | 3.6 | 3.4 | 0.4 | 0.1 | 2.8 | 3.3 | 3.9 | 4.3 | 3.1 | 4.1 |
| September | 4.7 | 4.6 | 0.3 | 0.1 | 4.1 | 4.5 | 4.8 | 5.3 | 4.3 | 5.2 |
| October | 5.9 | 5.9 | 0.8 | 0.1 | 3.9 | 5.5 | 6.4 | 7.0 | 4.4 | 6.9 |
| November | 6.8 | 7.0 | 0.4 | 0.1 | 5.7 | 6.7 | 7.1 | 7.5 | 6.0 | 7.4 |
| December | 7.0 | 7.2 | 0.5 | 0.1 | 5.4 | 6.7 | 7.4 | 7.7 | 6.1 | 7.7 |
| (c)Tolar Grande | | | | | | | | | | |
| January | 7.9 | 7.9 | 0.7 | 0.1 | 6.5 | 7.4 | 8.5 | 8.9 | 6.7 | 8.8 |
| February | 7.7 | 7.7 | 0.5 | 0.1 | 6.2 | 7.5 | 8.0 | 8.2 | 6.5 | 8.2 |
| March | 6.0 | 6.0 | 1.2 | 0.2 | 2.3 | 5.8 | 6.8 | 7.3 | 3.7 | 7.2 |
| April | 4.7 | 4.5 | 0.7 | 0.1 | 3.6 | 4.2 | 5.2 | 5.7 | 3.6 | 5.7 |
| May | 3.2 | 3.2 | 0.3 | 0.1 | 2.4 | 3.1 | 3.3 | 3.9 | 2.6 | 3.8 |
| June | 2.8 | 2.7 | 0.2 | 0.1 | 2.4 | 2.6 | 2.9 | 3.1 | 2.5 | 3.0 |
| July | 2.7 | 2.7 | 0.4 | 0.1 | 1.8 | 2.4 | 3.0 | 3.4 | 1.9 | 3.3 |
| August | 3.8 | 3.6 | 0.5 | 0.1 | 2.6 | 3.6 | 4.2 | 4.7 | 3.1 | 4.6 |
| September | 5.0 | 5.0 | 0.7 | 0.1 | 2.0 | 4.8 | 5.3 | 5.9 | 4.3 | 5.7 |
| October | 6.4 | 6.7 | 0.7 | 0.1 | 4.1 | 6.2 | 6.8 | 7.1 | 5.0 | 7.1 |
| November | 7.3 | 7.4 | 0.4 | 0.1 | 6.1 | 7.3 | 7.6 | 7.8 | 6.5 | 7.7 |
| December | 8.3 | 8.4 | 0.4 | 0.1 | 6.6 | 8.2 | 8.5 | 8.7 | 8.1 | 8.6 |

minima show a mean value of 98% in Salta, 18% in El Rosal, and 53% in Tolar Grande, indicating that these minimum values represent unusual extreme values of $I_T$. This is also shown by the comparison between the $P_5$ and the minima, with differences higher than 100% for some months (e.g., 121% in July in Salta and 132% in September in Tolar Grande). However, the differences between the $Q_3$ and the maxima show a mean value of 14% in Salta, 6% in El Rosal, and 5% in Tolar Grande, indicating that these maximum values can be considered representative of $I_T$ in El Rosal and Tolar Grande, but less representative in Salta. This is also shown by the comparison between the $P_{95}$ and the maxima, with no difference between these values for some months (e.g., in May in both El Rosal and Tolar Grande).

The $I_{UVER}$ mean values vary from 1.9 to 6.1 $kJ\,m^{-2}$ in Salta, 2.5–7.3 $kJ\,m^{-2}$ in El Rosal, and 2.7–8.3 $kJ\,m^{-2}$ in Tolar Grande. These are also considerably higher in El Rosal (16–29%) and Tolar Grande (22–33%) than those obtained in Salta. The maximum values are observed in January (Salta and El Rosal) and December (Tolar Grande), whereas the minimum values are observed in June (Salta and El Rosal) and July (Tolar Grande). The values of the mean and the median are similar, with the difference between them being less than 5% of the mean value in El Rosal and Tolar Grande, and less than 11% in Salta. The standard deviation shows values of 0.9 $kJ\,m^{-2}$ (23% of the mean value) in Salta, 0.5 $kJ\,m^{-2}$ (10%) in El Rosal, and 0.6 $kJ\,m^{-2}$ (10%) in Tolar Grande. The observed values of the standard deviation and the difference between the mean and the median are much higher in Salta than in the other two measurement sites. As explained before, this is probably due to El Rosal and Tolar Grande being located at a much higher altitude than Salta, making atmospheric attenuation factors, such as cloudiness or aerosols, to be more significant in Salta than in the other two measurement sites.

The comparison of the extreme values of $I_{UVER}$ with their corresponding quartile values shows mean values of 80% in Salta, 19% in El Rosal, and 46% in Tolar Grande for the differences between the $Q_1$ and the minima, which indicates that these minimum values represent unusual extreme values of $I_{UVER}$. This is also shown by the comparison between the $P_5$ and the minima, with great differences for some months (e.g., 83% in July in Salta and 61% in March in Tolar Grande). The mean values for the differences between the $Q_3$ and the maxima are 15% in Salta, 8% in El Rosal, and 7% in Tolar Grande, indicating that these maximum values can be considered representative of $I_{UVER}$ in El Rosal and Tolar Grande, but less representative in Salta. This is also shown by the comparison between the $P_{95}$ and the maxima, showing no difference between these values for some months (e.g., in April, June, and December in El Rosal, and February, April, and October in Tolar Grande).

Therefore, the results obtained for both $I_T$ (in $MJ \cdot m^{-2}$) and $I_{UVER}$ (in $kJ \cdot m^{-2}$) show a similar behavior, with maximum and minimum values observed in the summer and winter, respectively, similar values of the mean and the median, and minimum values representing unusual extreme values while the maximum values are at some level representative of $I_T$ and $I_{UVER}$. The observed differences between the measurement stations are also similar for both

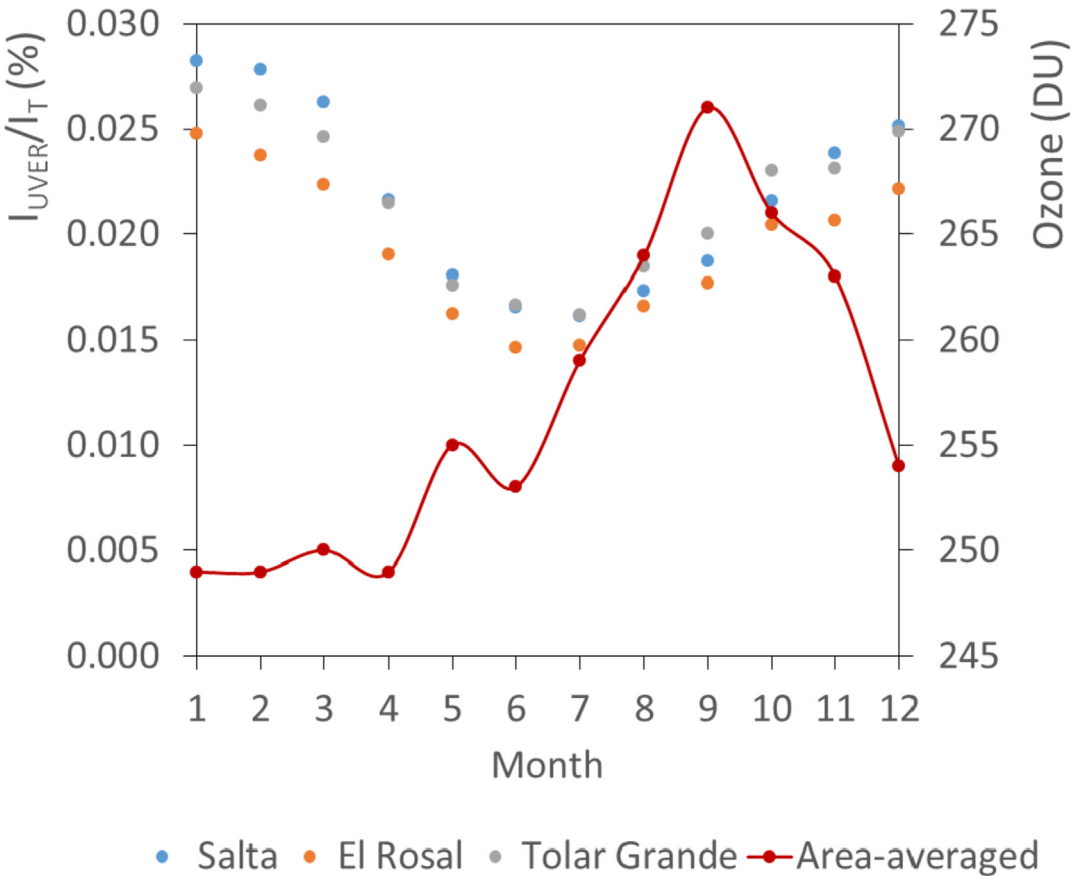


**Fig. 2.** Annual evolution of the monthly mean values of the $I_{UVER}/I_T$ ratio and the area-averaged total ozone column over the study region in: a) Salta, b) El Rosal, and c) Tolar Grande.

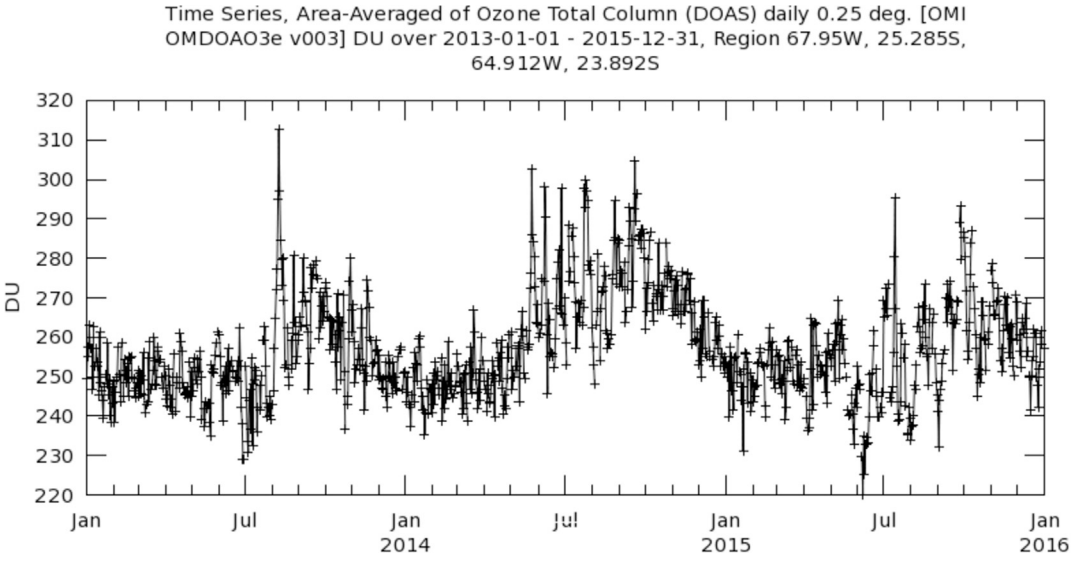


**Fig. 3.** Time evolution of area-averaged total ozone column measured by OMI over the study region during the period 2013–2015.

spectral ranges.

### 2.2. Relationship between $I_T$ and $I_{UVER}$

For the three measurement sites, the $I_{UVER}/I_T$ ratio has been estimated, and the annual evolution of its monthly mean values is shown in Fig. 2. The evolution shows no symmetry with respect to the central annual minimum in June, being the monthly mean values of the $I_{UVER}/I_T$ ratio higher during the first half of the year. This is related to the annual evolution of the total ozone column, which reaches minimum values in autumn and maximum values in spring, as can be observed in Fig. 2, which also shows the annual

**Table 4**
Parameters of the linear regression $I_{UVER} = m\ I_T + n$ for daily values obtained in each measurement site: a) Salta, b) El Rosal, and c) Tolar Grande.

| | m ($\times 10^{-4}$) | n (kJ/m$^2$) | $R^2$ | Altitude (m) |
|---|---|---|---|---|
| Salta | $2.48 \pm 0.07$ | $-0.4 \pm 0.1$ | 0.77 | 1190 |
| El Rosal | $3.01 \pm 0.06$ | $-2.6 \pm 0.1$ | 0.89 | 3355 |
| Tolar Grande | $3.23 \pm 0.05$ | $-0.3 \pm 0.1$ | 0.92 | 3560 |

evolution of the monthly mean values of the area-averaged total ozone column over the study region. This behavior of the total ozone column can also be observed in Fig. 3, which shows the evolution of the area-averaged total ozone column over the study region during the period 2013–2015, and it has a great impact on $I_{UVER}$ while it has nearly no effect over $I_T$ [38–40]. The data used in Figs. 2 and 3 was obtained from NASA's OMI through Giovanni (http://disc.sci.gsfc.nasa.gov/giovanni).

Since $I_T$ is usually measured in most meteorological stations around the world, but $I_{UVER}$ is not, it could be useful to be able to derive $I_{UVER}$ values from $I_T$ measurements. Therefore, following previous studies [24,41–46], the relationship between the daily values of $I_{UVER}$ and $I_T$ has been fitted to a linear regression ($I_{UVER} = m\ I_T + n$). The intercept of the linear regression should be considered an estimation of the offset between the $I_{UVER}$ and $I_T$ datasets. The linear regressions obtained in each measurement site are shown in Table IV. The results show good correlation between $I_{UVER}$ and $I_T$, with values of the correlation coefficient $R^2$ approximately of 0.90 in El Rosal (0.89) and Tolar Grande (0.92), whereas in Salta is lower (0.77).

The linear regressions shown on Table IV seem to suggest that the $I_{UVER}/I_T$ ratio increases with altitude. Fig. 4 shows the relationship between the slopes of the linear regressions $I_{UVER} = m\ I_T + n$ and the altitude obtained in this study for the three measurement sites, as well as that obtained in previous works in Esfahan (Iran) [26] and in 16 locations in Spain [47]. This relationship has been fitted to a linear regression ($I_{UVER}/I_T = m\ ALTITUDE + n$), and the results show good correlation, with a value of the correlation coefficient of $R^2 = 0.86$. The slope of this linear regression has a value of $0.32 \pm 0.03$ units of the $I_{UVER}/I_T$ ratio per km, which indicates that the influence of altitude on $I_{UVER}$ is more significant than on $I_T$. This value would allow to estimate the $I_{UVER}/I_T$ ratio for a site of known altitude, and then $I_{UVER}$ could be easily derived from $I_T$ measurements in those sites located at high altitudes which routinely measure $I_T$ but not $I_{UVER}$.

### 2.3. Relationship between $k_{TUVER}$ and $k_T$

The clearness index, $k_T$, is defined as the ratio between the total irradiance over a horizontal surface, I, and the total horizontal

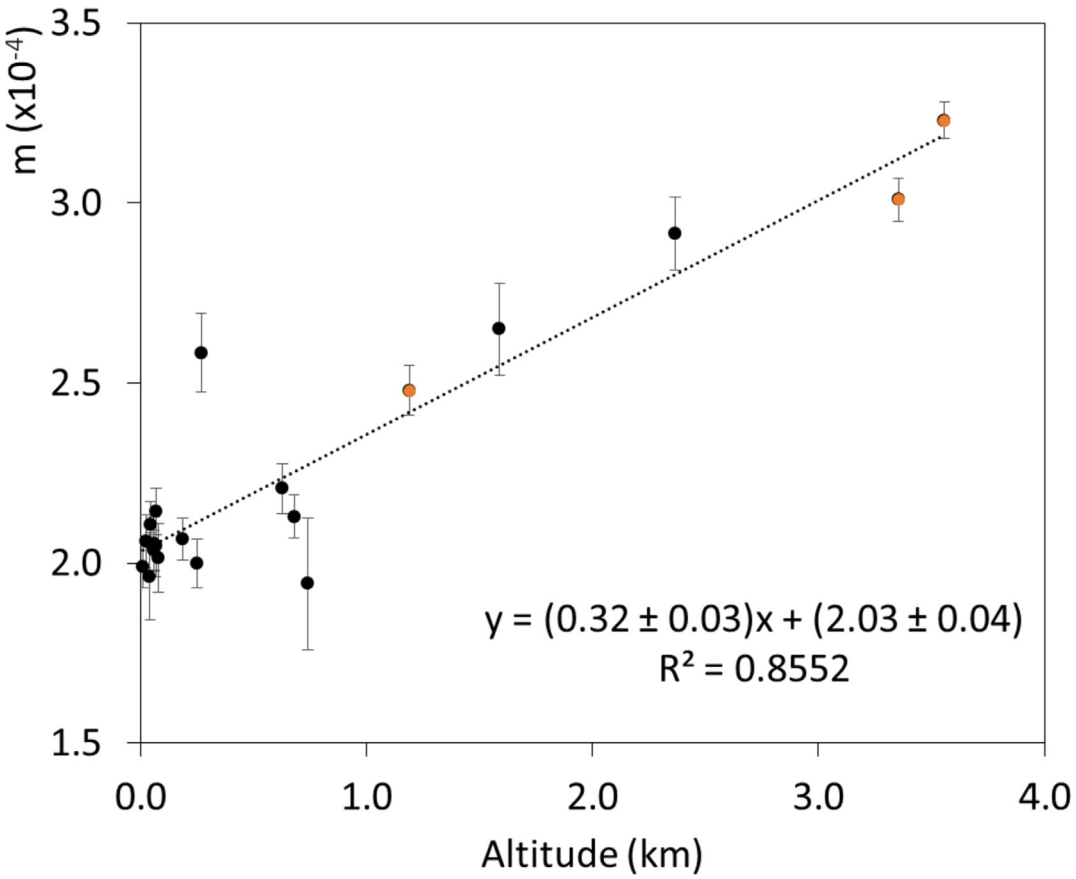


**Fig. 4.** Relationship between the slopes of the linear regression $I_{UVER} = mI_T + n$ and site altitude obtained in Salta, El Rosal, and Tolar Grande (orange points) and in Esfahan (Iran) [26], and 16 Spanish locations [41] (black points).

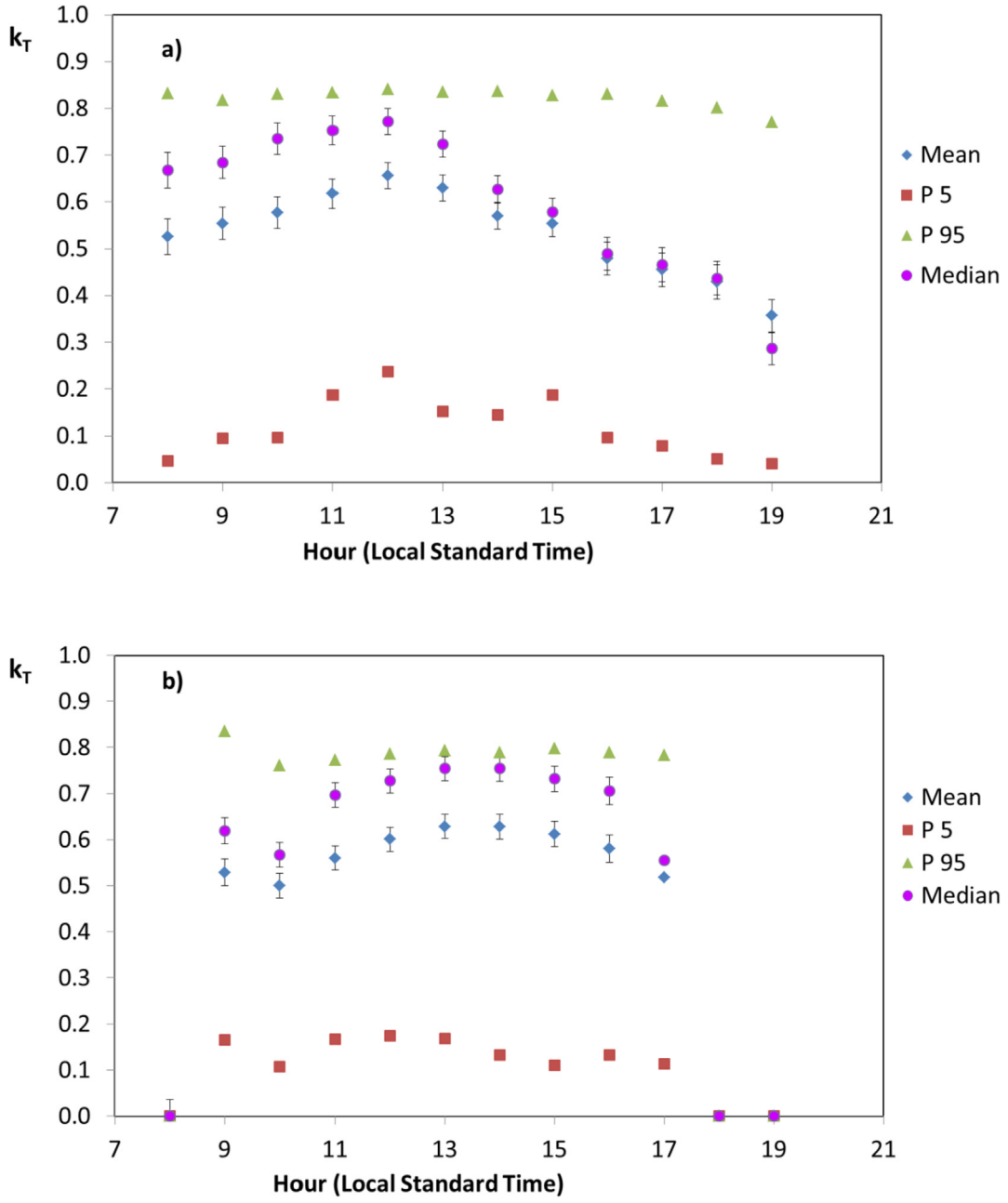


**Fig. 5.** Hourly mean, median, and percentiles P5 and P95 of $k_T$ versus time in Salta in: a) December, and b) June.

irradiance on the top of the atmosphere, $I_0$ [48]:

$$k_T = \frac{I}{I_0} = \frac{I}{I_{SC}\rho^{-2}\cos(\theta_Z)} \quad (1)$$

where $I_{SC}$ is the solar constant (1367 W m$^{-2}$), $\rho^{-2}$ is a factor that accounts for the day by day correction for the Sun–Earth distance and $\Theta_z$ is the solar zenith angle. The clearness index decreases when the atmospheric attenuation increases, mainly due to cloudiness.

Thus, an erythemal clearness index, $k_{TUVER}$, can be defined as well in the UV erytemal irradiance (UVER) spectral range [49]:

$$k_{TUVER} = \frac{UVER}{I_{SCUVER}\rho^{-2}\cos(\theta_Z)} \quad (2)$$

where $I_{SCUVER}$ is the solar constant in the UVER range (9.89 W m$^{-2}$), which has been obtained from the SUSIM ATLAS spectral data (http://wwwsolar.nrl.navy.mil/susim_atlas_data.html). Both UVER and $I_{SCUVER}$ are determined as the spectrally integrated weighted solar irradiance at ground level with the spectral standard erythema action curve adopted by the CIE in 1987 [19]. $\rho^{-2}$ and $\Theta_z$ take the same meaning as in Equation (1).

Although the clearness indices are strictly defined from instantaneous values, they have also been used with hourly [24,37,41,47], daily [43,50–52] and monthly [23,52,53] data. In this

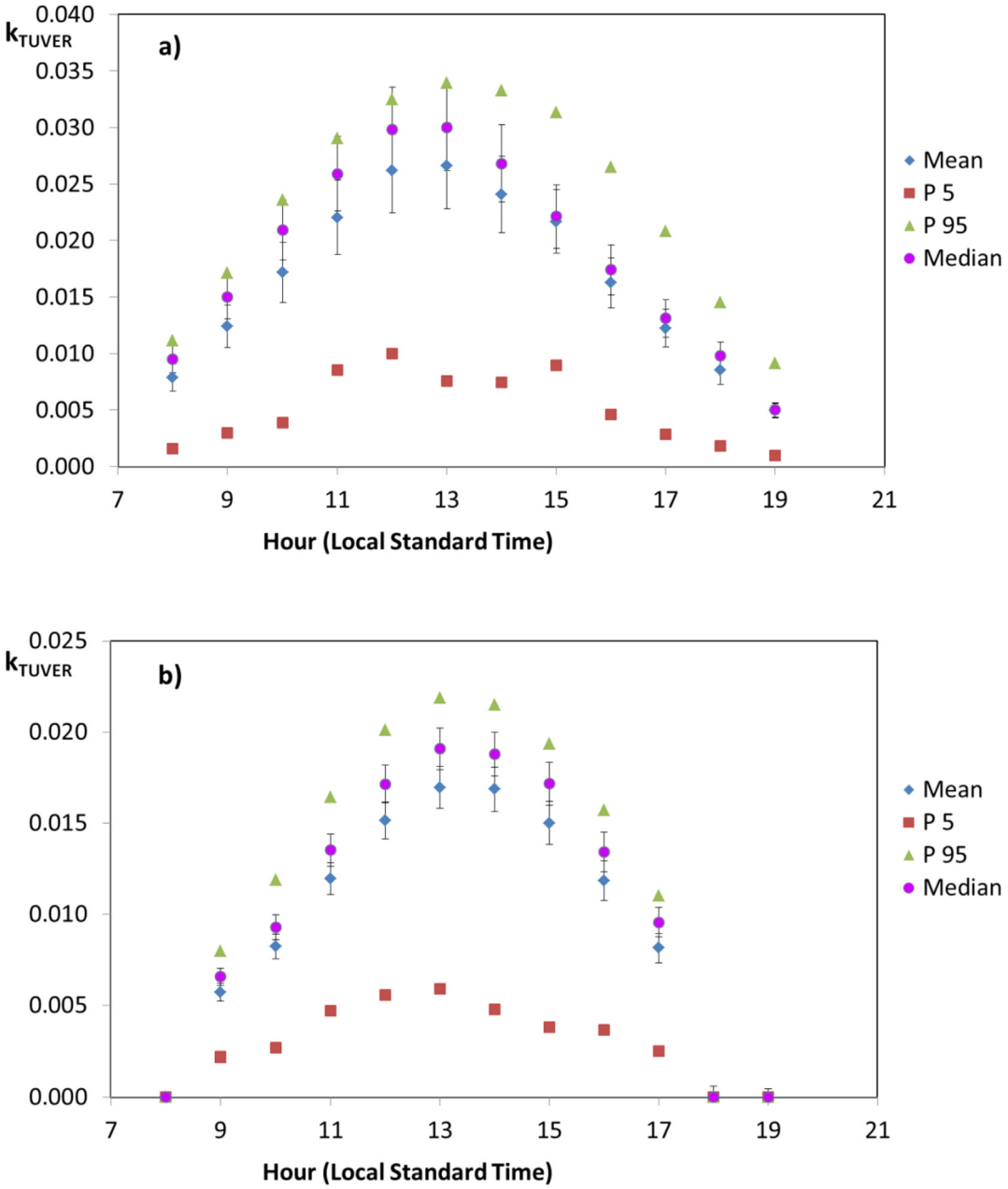


**Fig. 6.** Hourly mean, median, and percentiles P5 and P95 of $k_{TUVER}$ versus time in Salta in: a) December, and b) June.

work, the $I_T$ and $I_{UVER}$ measurements recorded at the three measurement sites have been used to estimate the hourly, daily and monthly values of the clearness indices $k_T$ and $k_{TUVER}$.

Figs. 5 and 6 show the mean, median, and the percentiles P5 and P95 of the hourly values of $k_T$ and $k_{TUVER}$, respectively, versus time in Salta. This analysis has been limited only to the months representing the typical situation in summer (December) and winter (June), and only the values for Salta are shown since those obtained in the other two measurement sites, El Rosal and Tolar Grande, behave in a very similar way. The hourly values of $k_T$ show a nearly unchanging distribution during the day, whereas $k_{TUVER}$ shows a clear hourly dependence. It is also observed that $k_T$ is nearly constant in summer and winter when the values corresponding to high zenith angles are not considered, while $k_{TUVER}$ is nearly twice in summer than in winter. These results agree with those obtained in a previous study for instantaneous values of clearness indices in Valencia (Spain) [37].

Figs. 7 and 8 show the annual evolution of $k_T$ and $k_{TUVER}$, respectively, during the period 2013–2015 in: a) Salta, b) El Rosal, and c) Tolar Grande. In this box diagram, the dividing segment in the box is the median. The top/bottom box limits represent the monthly median plus/minus the Q1/Q3. The box bars represent the percentiles P5 and P95. Minimum and maximum values are represented by crosses.

The monthly average value of $k_T$ is much higher in El Rosal and Tolar Grande than in Salta, ranging from 0.44 to 0.54 in Salta, from 0.64 to 0.79 in El Rosal, and from 0.68 to 0.78 in Tolar Grande. The monthly average value of $k_T$ shows no seasonal dependence, with the minimum and maximum values being obtained during the summer months (November, December, and January) in El Rosal

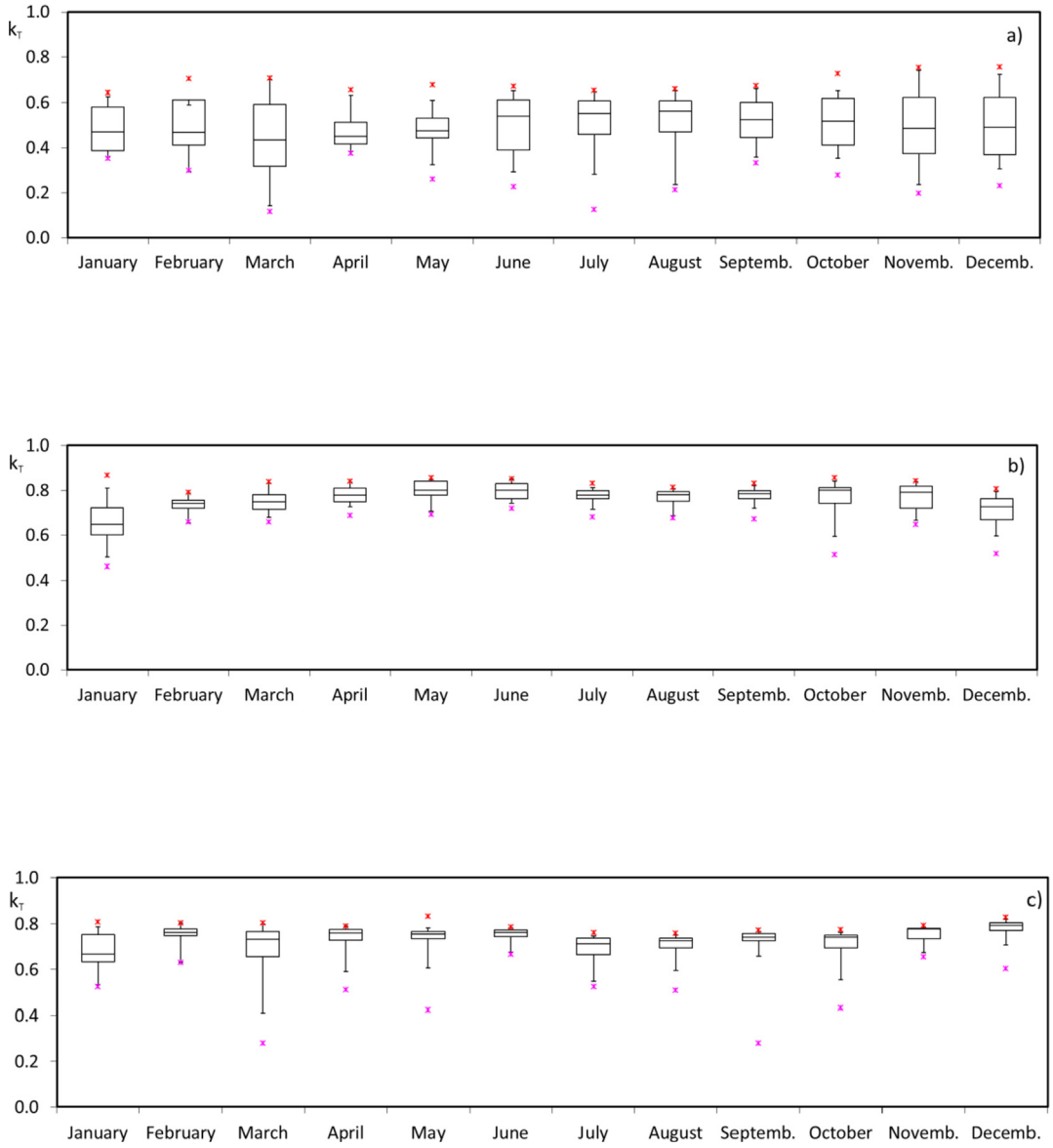


**Fig. 7.** Monthly statistics of daily $k_T$ during the period 2013–2015 in: a) Salta, b) El Rosal, and c) Tolar Grande. The dividing segment in the box is the median. The top/bottom box limits represent the monthly median plus/minus the Q1/Q3. The box bars represent the percentiles P5 and P95. Minimum and maximum values are represented by crosses.

and Tolar Grande, whereas in Salta the minimum is obtained in March and the maximum in July. Moreover, the monthly mean value (±standard deviation) of $k_T$ for the entire period is: $0.5 \pm 0.2$ in Salta, $0.75 \pm 0.16$ in El Rosal, and $0.72 \pm 0.12$ in Tolar Grande. The values of $k_T$ obtained in El Rosal and Tolar Grande are much higher than those obtained in Salta, because $k_T$ increases significantly with altitude [54]. When comparing the monthly mean values obtained for the entire period, the increase of $k_T$ with altitude has a value of 0.12 and 0.09 units per km in El Rosal and Tolar Grande, respectively.

The monthly average value of $k_{TUVER}$ ranges from 0.011 to 0.018 in Salta, from 0.014 to 0.022 in El Rosal, and from 0.014 to 0.024 in Tolar Grande. $k_{TUVER}$ shows a clear seasonal dependence, with the minimum values being obtained during the winter months (June and July) and the maximum values during the summer months (December and January) in the three measurement sites. Moreover, the monthly mean value (±standard deviation) of $k_{TUVER}$ for the entire period is: $0.014 \pm 0.008$ in Salta, $0.019 \pm 0.008$ in El Rosal, and $0.020 \pm 0.008$ in Tolar Grande. The values of $k_{TUVER}$ obtained in El Rosal and Tolar Grande are also higher than those obtained in Salta. When comparing the monthly mean values obtained for the entire period, the increase of $k_{TUVER}$ with altitude has a value of 0.0023 and 0.0025 units per km in El Rosal and Tolar Grande, respectively.

In order to establish a relationship between $k_T$ and $k_{TUVER}$, a multivariable regression of $k_{TUVER}$ as a function of the solar zenith angle, $\theta_z$, and $k_T$ has been performed, assuming a linear dependence of $k_{TUVER}$ with these two variables. The dependence of $k_{TUVER}$ with $\theta_z$ is included in this regression since both the UV erythemal and broadband spectral ranges have different responses to the absorption by ozone with increasing $\theta_z$ [47]. Besides, random perturbations of $\theta_z$ and $k_T$ are considered independent between them. Since the three measurement sites are relatively close to each other, the total ozone column over them is homogeneous (the difference between the monthly mean values of the total ozone column is

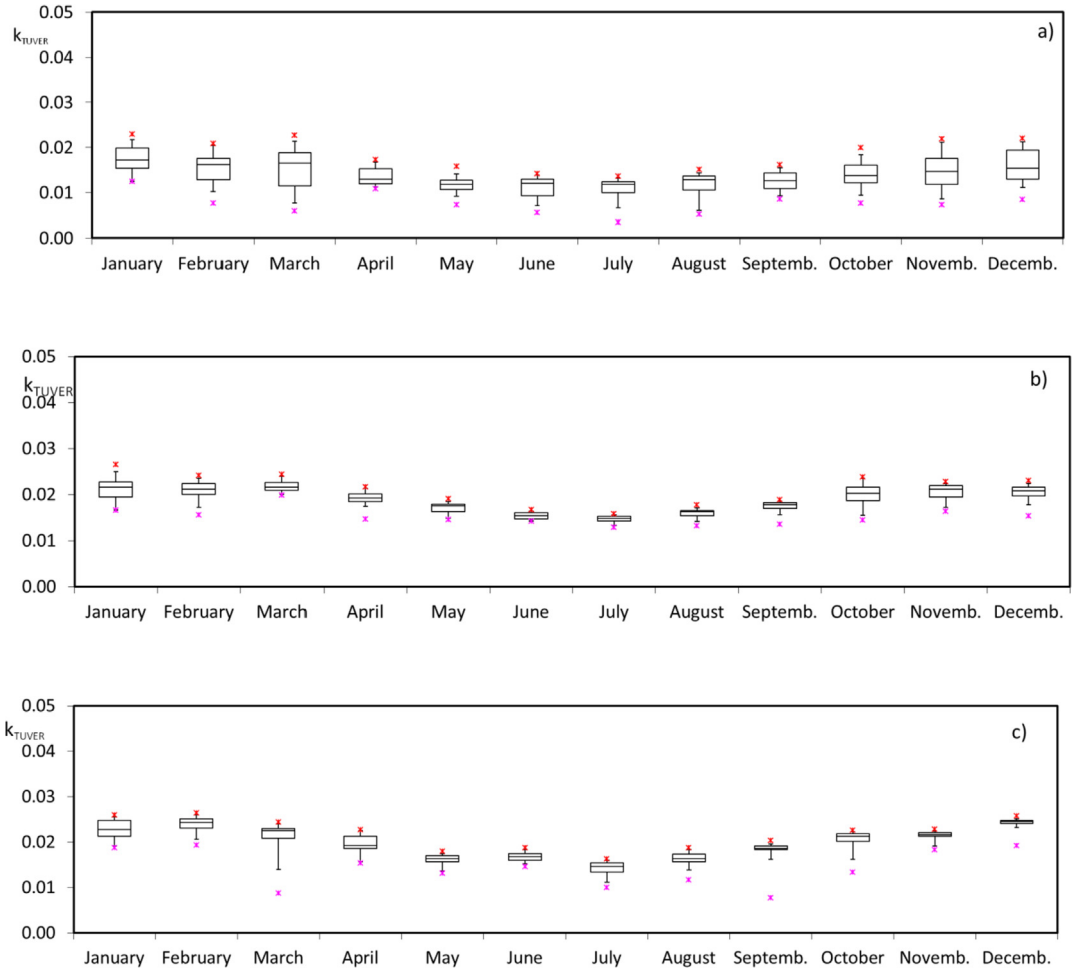


**Fig. 8.** Monthly statistics of daily $k_{TUVER}$ during the period 2013–2015 in: a) Salta, b) El Rosal, and c) Tolar Grande. The dividing segment in the box is the median. The top/bottom box limits represent the monthly median plus/minus the Q1/Q3. The box bars represent the percentiles P5 and P95. Minimum and maximum values are represented by crosses.

always equal or less than 5 DU), and thus this variable has not been included in the multivariable regression. However, for studies in larger regions, the total ozone column should also be considered when performing the multivariable regression since UVER is partly absorbed by ozone. Since the difference in the latitude of the three measurement sites is less than 0.5°, this variable has not been included in the multivariable regression. The multivariable regressions obtained in each measurement site are the following:

$$\text{Salta: } k_{TUVER} = -0.00024\ \theta_z + 0.022\ k_T + 0.014\ (R^2 = 0.89) \quad (3)$$

$$\text{El Rosal: } k_{TUVER} = -0.00034\ \theta_z + 0.020\ k_T + 0.020\ (R^2 = 0.90) \quad (4)$$

$$\text{Tolar Grande: } k_{TUVER} = -0.00040\ \theta_z + 0.020\ k_T + 0.025\ (R^2 = 0.95) \quad (5)$$

These results show a good correlation between $k_{TUVER}$ and the variables $\theta_z$ and $k_T$ and the regression coefficients obtained for $k_T$ are similar in the three measurement sites (0.22 in Salta, and 0.20 in El Rosal and Tolar Grande), showing the reduction in the local nature of the relationship between UVER and broadband solar radiation of these multivariable regressions. These expressions allow to estimate the not so commonly measured $k_{TUVER}$ from $k_T$, which is usually derived from variables commonly measured in most radiation measurement sites around the world, and $\theta_z$. The obtained values of the correlation coefficient $R^2$ are 0.89 in Salta, 0.90 in El Rosal, and 0.95 in Tolar Grande.

## 3. Conclusions

The broadband solar irradiation, $I_T$, and the erythemal UV irradiation, $I_{UVER}$, measured from 2013 to 2015 at three sites located in the Salta Province in Northwestern Argentina at high altitudes between 1190 and 3560 m a.s.l (Salta, El Rosal, and Tolar Grande) have been studied in order to determine a relationship which would allow to estimate $I_{UVER}$ from $I_T$. This relationship is especially important in those places where $I_{UVER}$ measurements are not available and adequate photoprotection measures are needed given their dense population and location at high altitude.

The relationship between the daily values of $I_{UVER}$ and $I_T$ has been fitted to a linear regression ($I_{UVER} = m\ I_T + n$), obtaining in the three measurement sites good correlation between $I_{UVER}$ and $I_T$, with values of the correlation coefficient $R^2 \geq 0.77$. Besides, since the $I_{UVER}/I_T$ ratio seems to increase with altitude, the relationship between this ratio and altitude has been fitted to a linear regression ($I_{UVER}/I_T$ = m ALTITUDE + n), which shows good correlation ($R^2 = 0.86$) and an increase of the $I_{UVER}/I_T$ ratio with altitude of $0.32 \pm 0.03$ units per km. This result, which indicates a more

significant influence of altitude on $I_{UVER}$ than on $I_T$, would allow to estimate the $I_{UVER}/I_T$ ratio for a site of known altitude, and since $I_T$ is usually measured in most meteorological stations around the world, $I_{UVER}$ could be easily derived too.

Given the local nature of the obtained relationship between $I_T$ and $I_{UVER}$, the dimensionless clearness indices $k_T$ and $k_{TUVER}$ have been estimated and analyzed. A multivariable regression of $k_{TUVER}$ as a function of the solar zenith angle, $\theta_z$, and $k_T$ has been performed, assuming a linear dependence of $k_{TUVER}$ with these two variables. The obtained regressions in the three measurement sites show good correlation between the variables ($R^2 \geq 0.89$) and similar regression coefficients for $k_T$, which indicate a reduction in the local nature of the relationship between UVER and broadband solar radiation.

## Acknowledgements

This work was financed by the cooperation project SN07A149 between the University of Valencia (Spain) and the University of Salta (Argentina). The Solar Radiation Group at the University of Valencia has been supported by the Spanish Ministry of Science and Innovation (MICINN) of Spain through projects CGL2015-70432 and CGL2015-64785, and by the Valencian Autonomous Government through the project PROMETEOII/2014/058. Analyses and visualizations used in Figs. 2 and 3 of this paper were produced with the Giovanni online data system, developed and maintained by the NASA GES DISC.

## References

[1] Commission Internationale de l'Éclairage (CIE). Standardization of the terms UV-A1, UV-A2 and UV-B. 1999. CIE 134/1 TC 6–26 report, Wien, Austria.
[2] Dotto M, Casati P. Developmental reprogramming by UV-B radiation in plants. Plant Sci 2017;264:96–101. https://doi.org/10.1016/j.plantsci.2017.09.006.
[3] San Z, K S-Y. Environmental occurrence and ecological risk assessment of organic UV filters in marine organisms from Hong Kong coastal waters. Sci Total Environ 2016;566(567):489–98. https://doi.org/10.1016/j.scitotenv.2016.05.120.
[4] Molins-Delgado D, Távora J, Díaz-Cruz MS, Barceló D. UV filters and benzotriazoles in urban aquatic ecosystems: the footprint of daily use products. Sci Total Environ 2018;601(602):975–86. https://doi.org/10.1016/j.scitotenv.2017.05.176.
[5] Jesper-Suhrhoff T, Scholz-Böttcher BM. Qualitative impact of salinity, UV radiation and turbulence on leaching of organic plastic additives from four common plastics - a lab experiment. Mar Pollut Bull 2016;102:84–94. https://doi.org/10.1016/j.marpolbul.2015.11.054.
[6] Nair S, Nagarajappa GB, Pandey KK. UV stabilization of wood by nano metal oxides dispersed in propylene glycol. J Photochem Photobiol B Biol 2018;183:1–10. https://doi.org/10.1016/j.jphotobiol.2018.04.007.
[7] Byrne C, Subramanian G, Pillai SC. Recent advances in photocatalysis for environmental applications. J Environ Chem Eng 2018;6:3531–55. https://doi.org/10.1016/j.jece.2017.07.080.
[8] Ameta R, Solanki MS, Benjamin S, Ameta S. Photocatalysis. In: Ameta S, Ameta R, editors. Advanced oxidation processes for waste water treatment. Academic Press; 2018. p. 135–75. https://doi.org/10.1016/B978-0-12-810499-6.00006-1.
[9] Monteiro RAR, Rodrigues-Silva C, Lopes FVS, Silva AMT, Boaventura RAR, Vilar VJP. Evaluation of a solar/UV annular pilot scale reactor for 24 h continuous photocatalytic oxidation of n-decane. Chem Eng J 2015;280:409–16.
[10] Lofrano G, Libralato G, Casaburi A, Siciliano A, Iannece P, Guida M, Pucci L, Dentice EF, Carotenuto M. Municipal wastewater spiramycin removal by conventional treatments and heterogeneous photocatalysis. Sci Total Environ 2018;624:461–9. https://doi.org/10.1016/j.scitotenv.2017.12.145.
[11] Sarkany RPE. Ultraviolet radiation and the skin. Reference module in earth systems and environmental sciences, 2018. Update of R.P.E. Sarkany ultraviolet radiation and the skin. Encyclop Environ Health 2011:469–82.
[12] Cavinato M, Jansen-Dürr P. Molecular mechanisms of UVB-induced senescence of dermal fibroblasts and its relevance for photoaging of the human skin. Exp Gerontol 2017;94:78–82. https://doi.org/10.1016/j.exger.2017.01.009.
[13] Bigagli E, Cinci L, D'Ambrosio M, Luceri C. Pharmacological activities of an eye drop containing *Matricaria chamomilla* and *Euphrasia officinalis* extracts in UVB-induced oxidative stress and inflammation of human corneal cells. J Photochem Photobiol B Biol 2017;173:618–25. https://doi.org/10.1016/j.jphotobiol.2017.06.031.
[14] Learn DB, Forbes PD, Sambuco CP. Photosafety assessment. In: Said Faqi Ali, editor. A comprehensive guide to toxicology in nonclinical drug development. second ed. Academic Press; 2017. p. 585–614. https://doi.org/10.1016/B978-0-12-803620-4.00022-0.
[15] Xu H, Elmets CA. UVB immunosuppression: vitamin D or not vitamin D? That is the question. J Invest Dermatol 2012;132:2676–8. https://doi.org/10.1038/jid.2012.327.
[16] Damiani E, Ullrich SE. Understanding the connection between platelet-activating factor, a UV-induced lipid mediator of inflammation, immune suppression and skin cancer. Prog Lipid Res 2016;63:14–27. https://doi.org/10.1016/j.plipres.2016.03.004.
[17] Lindqvit PG, Landin-Olsson M. The relationships between sun exposure and all-cause mortality. Photochem Photobiol Sci 2016;16:354–61.
[18] Schmitt J, et al. Is ultraviolet exposure acquired at work the most important risk factor for cutaneous squamous cell carcinoma? Results of the population-based case–control study FB-181. Br J Dermatol 2018;178:462–72.
[19] ISO 17166 CIE S 007/E. Erythema reference action spectrum and standard erythema dose. Wien, Austria: CIE Publications; 2000.
[20] Jacovides CP, Assimakopoulos VD, Tymvios FS, Theophilou K, Asimakopoulos DN. Solar global UV (280–380nm) radiation and its relationship with solar global radiation measured on the island of Cyprus. Energy 2006;31:2728–38.
[21] Kudish AI, Evseev E. Statistical relationships between solar UVB and UVA radiation and global radiation measurements at two sites in Israel. Int J Climatol 2000;20:759–70.
[22] Kudish AI, Evseev E. The analysis of solar UVB radiation as a function of solar global radiation, ozone layer thickness and aerosol optical density. Renew Energy 2011;36:1854–60.
[23] Kudish AI, Lyubansky V, Evseev EG, Ianetz A. Statistical analysis and intercomparison of the solar UVB, UVA and global radiation for beer sheva and Neve Zohar (Dead sea), Israel. Theor Appl Climatol 2005;80:1–15.
[24] Cañada J, Pedros G, Bosca JV. Relationships between UV (0.290–0.385 μm) and broad band solar radiation hourly values in Valencia and Córdoba, Spain. Energy 2003;28:199–217.
[25] Cañada J, Esteve AR, Marín MJ, Utrillas MP, Tena F, Martínez-Lozano JA. Study of erythemal, UV (A+B) and global radiation in Valencia (Spain). Int J Climatol 2008;28:693–902.
[26] Sabziparvar AA. Estimation of clear-sky effective erythema radiation from broadband solar radiation (300–3000 nm) data in an arid climate. Int J Climatol 2009;29:2027–32.
[27] De Miguel A, Roman R, Bilbao J, Mateos D. Evolution of erythemal and total shortwave solar radiation in Valladolid, Spain: effects of atmospheric factors. J Atmos Sol Terr Phys 2011;73:578–86.
[28] De Miguel A, Mateos D, Bilbao J, Roman R. Sensitivity analysis of ratio between ultraviolet and total shortwave solar radiation to cloudiness, ozone, aerosols and precipitable water. Atmos Res 2011;102:136–44.
[29] Wang L, Gong W, Luo M, Wang W, Hu B, Zhang M. Comparison of different UV models for cloud effect study. Energy 2015;80:695–705.
[30] Antón M, Serrano A, Cancillo ML, García JA. Relationship between erythemal irradiance and total solar irradiance in South-Western Spain. J Geophys Res 2008;113:D14208.
[31] Cede A, Luccini E, Nuñez L, Piacentini RD, Blunthaler M. Effects of clouds on erythemal and total irradiance as derived from data of the Argentine Network. Geophys Res Lett 2002;24(29):2223.
[32] Palancar GG, Toselli BM. Effects of meteorology on the anual and interanual cycle of the UVB and total radiation in Cordoba City, Argentina. Atmos Environ 2004;38:1073–82.
[33] McKenzie RL, Paulin KJ, Kotkamp M. Erythemal UV irradiances at Lauder, New Zealand: relationship between horizontal and normal incidence. Photochem Photobiol 1997;66:683–9.
[34] Zaratti F, Piacentini RD, Guillén HA, Cabrera SH, Liley JB, McKenzie RL. Proposal for a modification of the UVI risk scale. Photochem Photobiol Sci 2014;13:980–5.
[35] Utrillas MP, Salazar G, Suarez H, Castillo J, Marín MJ, Esteve AR, Martínez-Lozano JA. Analysis of UVER experimental irradiance and UV index at three different locations in Northwestern Argentina. J Photochem Photobiol B 2016;163:290–5.
[36] Vilaplana JM, Cachorro VE, Sorribas M, Luccini E, de Frutos AM, Berjon A, de la Morena B. Modified calibration procedures for a Yankee Environmental System UVB-1 biometer based on spectral measurements with a Brewer spectrophotometer. Photochem Photobiol 2006;82:508–11.
[37] Tena F, Martínez-Lozano JA, Utrillas MP, Marín MJ, Esteve AR, Cañada J. The erythemal clearness index for Valencia, Spain. Int J Climatol 2009;29:147–55.
[38] Adam MEN. Effect of stratospheric ozone in UVB solar radiation reaching the Earth's surface at qena, Egypt. Atmos Pollut Res 2010;1:155–60.
[39] Esteve AR, Martínez-Lozano JA, Marin MJ, Estellés V, Tena F, Utrillas MP. Influence of the ozone and the aerosols over experimental values of UVER a ground level, at Valencia. Int J Climatol 2009;29:2171–82. https://doi.org/10.1002/joc.1847.
[40] Antón M, Serrano A, Cancillo ML, García JA. Relationship between erythemal irradiance and total solar irradiance in South-Western Spain. J Geophys Res 2008:113. https://doi.org/10.1029/2007JD009627.
[41] Ogunjobi KO, Kim YJ. Ultraviolet (0.280-0.400 μm) and broadband solar hourly radiation at Kwangju, South Korea: analysis of their correlation with

aerosol optical depth and clearness index. Atmos Res 2004;71:193–214.
[42] Martínez-Lozano JA, Tena F, Utrillas MP. Ratio of UV to global broad band irradiation in Valencia, Spain. Int J Climatol 1999;19:983–91.
[43] Martínez-Lozano JA, Casanovas AJ, Utrillas MP. Comparison of global ultraviolet (290-385 nm) and global irradiation measured during the warm season in Valencia, Spain. Int J Climatol 1994;14:93–102.
[44] Ilyas M, Pandy A, Hassan SIS. UV-B radiation at Penang. Atmos Res 1999;51:141–52.
[45] Basset HA, Korany MH. The global and UV-B radiation over Egypt. Atmósfera 2007;20:341–58.
[46] Jacovides CP, Tymvios FS, Asimakopoulos DN, Kaltsounides NA, Theoharatos GA, Tsitouri M. Solar global UVB (280–315 nm) and UVA (315–380 nm) radiant fluxes and their relationships with broadband global radiant flux at an eastern Mediterranean site. Agric For Meteorol 2009;149:1188–200.
[47] Gandía S, Utrillas MP, Gómez-Amo JL, Esteve AR, Estellés V, Pedrós R, Núñez JA. Martínez Lozano JA. Relationship between UVB and broadband solar radiation in Spain. Int J Climatol 2015;35:1761–71.
[48] Liu BYH, Jordan RC. The interrelationship and characteristic distribution of direct, diffuse and total solar radiation. Sol Energy 1960;4:1–19.
[49] Alados-Arboledas L, Alados I, Foyo-Moreno I, Olmo FJ, Alcántara A. The influence of clouds on surface UV erythemal irradiance. Atmos Res 2003;66:273–90.
[50] Santos JM, Pinazo JM, Cañada J. Methodology for generating daily clearness index values $K_T$ starting from the monthly average daily value. Determining the daily sequence using stochastic models. Renew Energy 2003;28:1523–44.
[51] Ulgen K, Hepbasli A. Prediction of solar radiation parameters through clearness index for Izmir, Turkey, Energ. Source 2002;24:773–85.
[52] Udo SO. Sky conditions at Ilorin as characterized by clearness index and relative sunshine. Sol Energy 2000;69:45–53.
[53] Kudish AI, Ianetz A. Analysis of daily clearness index, global and beam radiation for Beer Sheva, Israel: partition according to day type and statistical analysis. Energy Convers Manag 1996;37:405–16.
[54] Salazar G, Raichijkc C. Evaluation of clear-sky conditions in high altitude sites. Renew Energy 2014;64:197–202.